Elastic Modulus Estimation based on Local Displacement Observation of Elastic Body

M. Morita, M. Nakao, *Member, IEEE*, and T. Matsuda, *Member, IEEE*

***Abstract*—A method is proposed that provides estimates of the spatial variation of elastic moduli using local displacements of the elastic body. A central issue of elastography imaging has been the limited area of measurement. With the proposed method, stiffness parameter estimations are considered as minimization problems using finite-element models. The sparseness of the gradient of tissue elasticity is also exploited to improve estimation accuracy. Simulation experiments show that based on a 5% area of observation of a simple plate model with non-uniform elasticity the spatial variation of Young's modulus is reconstructed to within 5% accuracy. This result suggests that the proposed framework significantly extends the area of estimation overcoming the limitations of conventional elastography techniques.**

I. Introduction

Tissue elasticity is an important characteristic in the medical field, because pathological changes of tissue are generally correlated with changes in tissue stiffness. Most kinds of tumor or lesion become harder than normal tissue as the disease progresses. By measuring tissue elasticity, a quantitative diagnosis based on mechanical properties of tissue is then possible. For this purpose, elastography [1] was developed in the 1990s to measure tissue elasticity and is replacing palpation performed by clinicians. In the interim, this technique has been widely investigated to quantify accurately the physical conditions of organs.

Elastography is a mode of imaging that enables tissue stiffness to be visualized and used to locate tumors or hard lesions in soft tissue. Ultrasound is widely used for elastography [2], particularly in the medical field for diagnosis. To date, two major approaches based on different types of measured physical quantities have been reported. One approach, strain elastography mapping, determines stiffness by analyzing the strain in tissue under stress [3]. It has the advantage of simple real-time measurements with high spatial resolution. However, accurate measurements of tissue stiffness are difficult because the magnitude of the applied external force is not proportional to the bio-tissue strain. Moreover, the method using focused acoustic radiation needs to apply external excitation to human bodies by strong convergent ultrasonic waves. Shear-wave elastography [4] is another approach providing a stiffness image by quantifying the propagation speed of the shear wave. Transient elastography is one such technique that is clinically available. However, transient elastography has the disadvantage in that measuring stiffness deep inside the body is difficult. A method that can measure deep-layer tissue stiffness non-invasively is therefore required.

To determine tissue stiffness and identify differing tissues, various methods have been reported. In [5], elastic modulus of tissue was estimated based on the Navier–Stokes equation by solving an optimization problem using a finite element (FE) model. Its mesh adaptation was also investigated to improve the accuracy of tissue-elasticity reconstruction [6]. As these methods show that elasticity reconstruction is possible for an observable area, no report has appeared investigating elasticity reconstruction that includes unobservable areas of elastic bodies. The models used in medical virtual reality simulators of organs [7, 8] require information of the elasticity of biological tissues. If such data could be obtained during surgery without additional hardware setup or burden, various areas of biomedical research and intraoperative support system [9] would benefit.

We hence propose a method based on local displacements of the observable area to estimate the spatial variation of elasticity over the entire elastic body. Stiffness parameters are reconstructed by solving a minimization problem using FE models. In addition, the sparseness of the gradient of tissue elasticity is introduced to improve estimation accuracy. This implementation has the possibility of extending the area of elasticity reconstruction, thereby overcoming the limitation of conventional elastography techniques. Also, a new application on vision-based elastography during surgery will be possible because internal elastic properties may be reconstructed from partial observations of deformed surfaces. We performed simulation experiments using a simple plate model with non-uniform elasticity. The results show that the proposed methods can estimate spatial variations of Young's modulus over the entire elastic body including unobservable areas. Details of the methods and experiments are described in Sections II and III, respectively.

II. Methods

A. Outline of the methods

As outlined in Fig. 1, the model assumes that the whole shape of the target elastic body is given, and a tetrahedral mesh can be configured for it. As CT or MRI imaging is available, this configuration is clinically acceptable. Here, we also assume that the elastic body has both observable and unobservable areas, and a point of contact is made in the observable area. This situation represents an external force being applied to a specific contact point on the elastic body, but the magnitude

M. Morita, M. Nakao, and T. Matsuda are with the Department of System Science, Kyoto University, Kyoto, Japan. (e-mail: {mmorita, megumi, tetsu}@i.kyoto-u.ac.jp).

978-1-5090-2809-2/17/$31.00 ©2017 IEEE

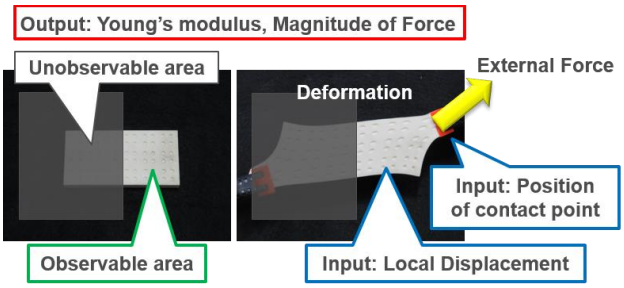

Figure 1. The concept of elastic modulus reconstruction based on observations of local displacements.

of the force is not given because the measurement of external forces is difficult in clinical situations during diagnosis or surgery. Because of recent advances in feature-based tracking [10] and image recognition algorithms, we can assume that displacements of some sampling points have occurred in the observable areas. We then estimate Young's moduli by solving a minimization problem based on these observed displacements. In the next two subsections, the problem is described and defined within the context of linear finite-element theory, and details of the proposed method are subsequently introduced.

B. Definition of the problem using linear finite-element theory

The FE model configured in simulations (Fig. 2) introduces an array of m observed vertices of a total of n vertices and a l-dimensional vector $\boldsymbol{E} = [E_0, E_1, \dots, E_{l-1}] \in \mathbb{R}^l$ of Young moduli. With $\boldsymbol{E}$, the FE mesh model is divided into l areas and we assume that each area has a unique Young modulus E_k $(k = 0, \dots, l-1)$. We define $\boldsymbol{f} \in \mathbb{R}^{3n}$ as the force applied to the vertices, $\boldsymbol{u} \in \mathbb{R}^{3n}$ the displacement of the vertices, and $K \in \mathbb{R}^{3n \times 3n}$ the stiffness matrix. Here, Young's moduli $\boldsymbol{E}$ are one of a set of parameters constituting K. Linear finite-element theory uses the following relation

$$\boldsymbol{f} = K\boldsymbol{u} \Leftrightarrow \boldsymbol{u} = K^{-1}\boldsymbol{f} = L\boldsymbol{f}. \qquad (1)$$

- Known quantities

1. Displacement of observed vertices

Since various methods to measure the displacement have been reported in previous studies, we assume that the displacement in an observable area is obvious. For example, surface deformations of elastic bodies based on camera images [10] and internal deformations based on ultrasonography [11] have been reported.

2. Positions of the contact points

Assuming that the elastic body is an organ, the force exerted by forceps or a transducer of probe can be considered as an external force. The area where the external force is applied such as contact points is obvious. We assume that Poisson's ratio and the positions of fixed vertices of the FE model are also obvious.

- Estimation targets

1. Young's modulus vector $\boldsymbol{E}$
2. External force vector $\boldsymbol{f}$

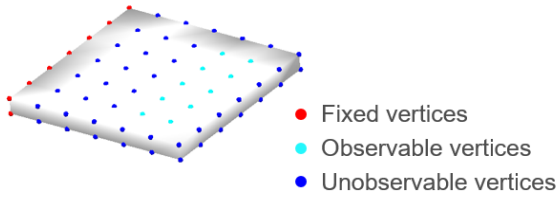

Figure 2. Simple plate mesh model with observable and unobservable areas.

C. Estimation method of Young's moduli solving the minimization problem

By labeling all vertices of the FE model as observed vertices by o or unobservable ones by i, (1) can be rewritten as

$$\begin{pmatrix} \boldsymbol{u_o} \\ \boldsymbol{u_i} \end{pmatrix} = \begin{pmatrix} L_{oo} & L_{oi} \\ L_{io} & L_{ii} \end{pmatrix} \begin{pmatrix} \boldsymbol{f_o} \\ \boldsymbol{f_i} \end{pmatrix}, \qquad (2)$$

where $\boldsymbol{u_o} \in \mathbb{R}^{3m}$ is a given vector quantity and $\boldsymbol{u_i}$ is an unknown vector. Extracting only that part related to $\boldsymbol{u_o}$ yields

$$\boldsymbol{u_o} = (L_{oo} \quad L_{oi}) \begin{pmatrix} \boldsymbol{f_o} \\ \boldsymbol{f_i} \end{pmatrix} = L_o(\boldsymbol{E})\boldsymbol{f}. \qquad (3)$$

The displacement of the observable vertices can be derived from (3). In observing multiple patterns of deformed shapes of the FE model, the pre-observed displacement matrix $\boldsymbol{U}_o \in \mathbb{R}^{3m \times \omega}$ is defined as

$$\boldsymbol{U}_o = [\boldsymbol{u}_{1o} \quad \boldsymbol{u}_{2o} \quad \cdots \quad \boldsymbol{u}_{\omega o}] \qquad (4)$$

where ω represents the number of patterns of the deformed shape of the FE model. The estimation method now involves updating $\boldsymbol{E}$ and $\boldsymbol{f}$ from initial values to those for which $\boldsymbol{u}'_o(\boldsymbol{E}, \boldsymbol{f})$ are closest to the observed displacement $\boldsymbol{u}_o$. The minimization problem based on $\boldsymbol{U}_o$ can now be stated; with its solution, $\boldsymbol{E}$ and $\boldsymbol{f}$ can then be estimated. We use the Covariance Matrix Adaptation Evolution Strategy (CMA-ES) [12] to solve the minimization problem,

$$\begin{aligned} \boldsymbol{E}^* &= \underset{\boldsymbol{E},\boldsymbol{f}}{\operatorname{argmin}} J(\boldsymbol{E}, \boldsymbol{f}) \\ &= \underset{\boldsymbol{E},\boldsymbol{f}}{\operatorname{argmin}} \left\| \boldsymbol{U}_o - \boldsymbol{U}'_o \right\|_F. \end{aligned} \qquad (5)$$

To improve the estimation accuracy, we focus on the sparseness of the gradient of tissue elasticity. Sparseness refers to the property of a matrix, the elements of which are mostly zero. As tumors or lesions are harder than normal tissue and confined, only a small region of the elastic body is hard, that is, the gradient of the tissue elasticity is sparse. By introducing the notion of sparsity, (5) is rewritten as

$$\begin{aligned} \boldsymbol{E}^* &= \underset{\boldsymbol{E},\boldsymbol{f}}{\operatorname{argmin}} J(\boldsymbol{E}, \boldsymbol{f}) \\ &= \underset{\boldsymbol{E},\boldsymbol{f}}{\operatorname{argmin}} \{ \left\| \boldsymbol{U}_o - \boldsymbol{U}'_o \right\|_F \\ &\qquad + \lambda \| \boldsymbol{E_0} - \boldsymbol{E} \|_1 \} \end{aligned} \qquad (6)$$

where λ is a parameter to control the sparseness of the gradient of elasticity. By considering sparseness, it is possible

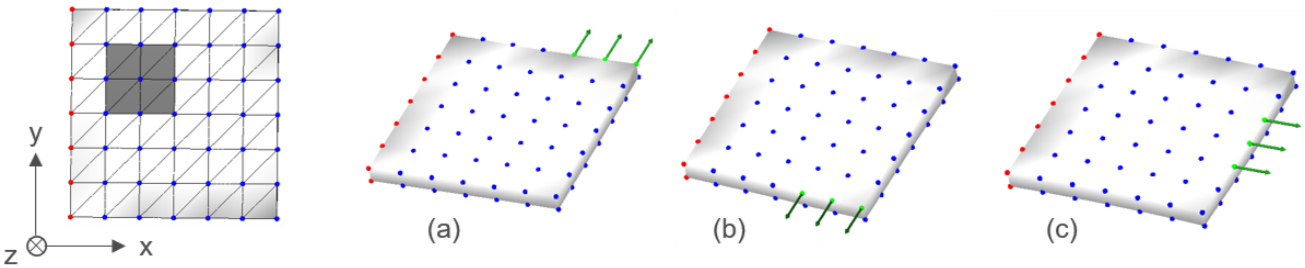

Figure 3. Boundary conditions for (a) force-1, (b) force-2, and (c) force-3. White area: 1.0 MPa, Grey area: 2.0 MPa. Red dots: fixed points, Blue dots: free points, Green dots: contact points of an external force.

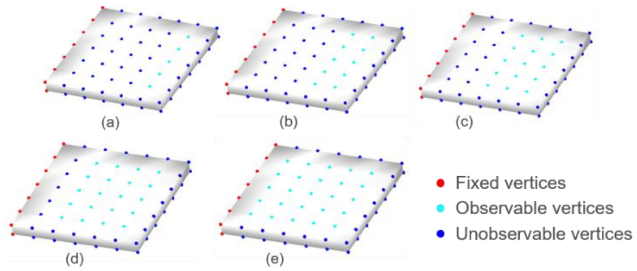

Figure 4. Setting of Observation condition.

to add a constraint condition whereby the elasticity in most areas of the elastic body is uniform, so that improvements in estimation accuracy can be expected.

III. Evaluation Experiment

A. Setting of experimental conditions

The purpose of this simulation is to verify how accurately the proposed method can estimate the spatial variation of elastic moduli and whether the area of elasticity reconstruction can be extended. We implemented the proposed method using Visual C/C++ and conducted simulation experiments on a computer (OS: Windows10 Professional, CPU: IntelCorei7-6700K, Memory: 16 GB).

1. Boundary condition

The FE model is configured with a mesh of 216 tetrahedra and 98 vertices. The positions of the fixed points and contact points are as indicated in Fig. 3; the number of fixed vertices is 14. We assume an external force using forceps or a transducer of a probe is exerted on the surface of an organ. The magnitude and direction of the external force is uniform over all neighboring vertices; specifically, at the contact points, a 10-N force is directed along (a) the -y axis, (b) the +y axis, and (c) the +x axis (Fig. 3). The number of observed vertices is set to (a) 5, (b) 10, (c) 15, (d) 20, (e) 25, and the number of observed vertices is incremented by 5 sequentially along the +x axis (Fig. 4).

2. Young's modulus $\boldsymbol{E}$

The FE mesh is divided into 36 equal parts and Young's modulus for each part is assumed to be that of normal tissue set at 1.0 MPa; the other parts are assumed to be the tumor with modulus 2.0 MPa (Fig. 3). In linear finite-element theory, the produce $L(\boldsymbol{E})$ with $\boldsymbol{f}$ for the observed displacement $\boldsymbol{u_o}$ is not uniquely determined. Therefore, we fix Young's modulus of the lower left part of the FE model in Fig. 3 to 1.0 and estimate Young's moduli as relative values. For the initial values in the estimation of Young's modulus, all elements of $\boldsymbol{E}$ are set to 1.0 and all elements of $\boldsymbol{f}$ are set to 0.0.

B. Evaluation experiment

In this section, we describe two experiments. Experiment 1 involved applying force-1 to FE model and estimating the spatial variation of Young's moduli based only on $\boldsymbol{u}_o(1)$, where $\boldsymbol{u}_o(i)$ is the displacement corresponding to force-i. In experiment 2, we focused on the pre-observed deformation patterns and sparseness of the gradient of the elasticity to improve estimation accuracy. In regard to the number of patterns, the more patterns we observed associated with the deformed shape of the elastic body, the more detail about the physical condition can be developed. Therefore, improvements in the estimation accuracy can be expected by solving the minimization problem based on a multiple number of observed displacements $\boldsymbol{u}_o$.

Denoting $\boldsymbol{E}$ as the original Young's modulus vector and $\boldsymbol{E}'$ as the estimated Young's modulus vector, the RMS is

$$RMS = \sqrt{\frac{1}{l}\sum_{i=0}^{l-1}\{(E'_i - E_i)^2\}} \qquad (7)$$

Simulations were performed 10 times, and $\boldsymbol{E}'$ with the smallest value $J(\boldsymbol{E}', \boldsymbol{f})$ in (5) were taken as representative values. From the result of experiment 1 [Fig. 5(a)], RMS decreases as the number of observed vertices increases. To estimate Young's moduli of this model with high accuracy, the number of observed vertices required was about 15.

For experiment 2, we pre-observed the displacements (i) $\boldsymbol{u}_o(1)$, (ii) $\boldsymbol{u}_o(1)$ and $\boldsymbol{u}_o(2)$, (iii) $\boldsymbol{u}_o(1)$ and $\boldsymbol{u}_o(2)$ and $\boldsymbol{u}_o(3)$, and set the coefficient λ in (6) to 0.0 (non-sparse) or 0.00003 (sparse). The results with (iii)-sparse are shown in Fig. 5(b) and by comparing with Fig. 5(a), it is obvious that our proposed approach to improve estimation accuracy is very effective. Fig. 5(c) represents the results of (i)-nonsparse, (i)-sparse, (ii)-nonsparse, (ii)-sparse, (iii)-nonsparse and (iii)-sparse for five observed vertices. From the results of Fig. 5(c), the RMS is reduced by about 0.1 MPa at the maximum by increasing the number of pre-observations, and RMS is reduced by about 0.45 MPa at the maximum by assuming sparseness in the gradient of elasticity.

From the result for the estimated values for Young modulus (Fig. 6), the spatial variation over the plate of the model was reconstructed to within 5% accuracy based on observations from just 5% of its area. As a result of this

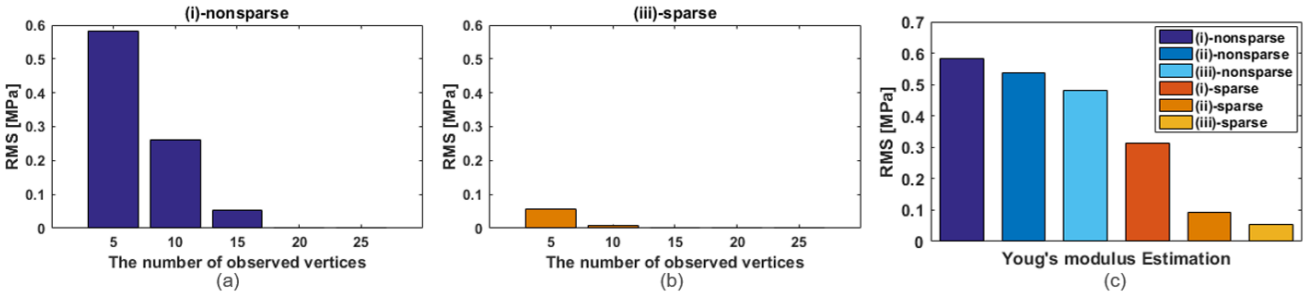

Figure 5. (a) (i)-nonsparse. (b) (iii)-sparse. (c) Comparison with results from five observed vertices.

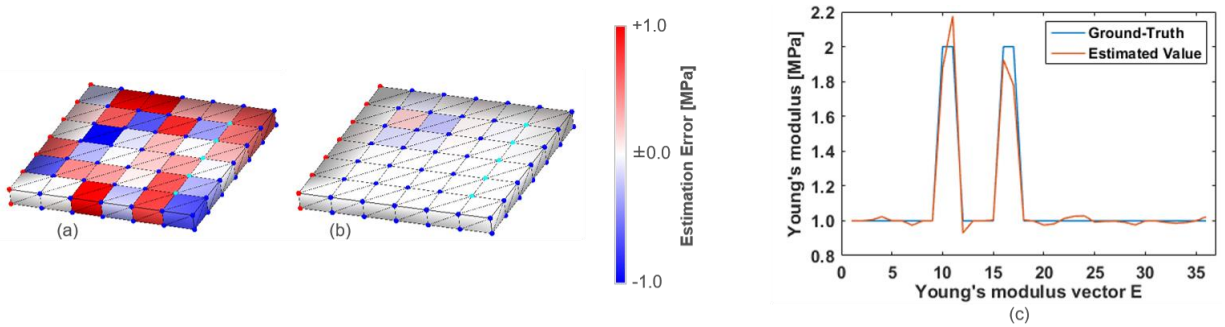

Figure 6. The number of observed vertices is 5. (a) Estimation error of (i)-nonsparse. (b) Estimation error of (iii)-sparse. (c) Estimated Young's moduli of (iii)-sparse.

simulation, our proposed method can estimate spatial variations of Young's modulus including unobservable areas based only on displacements measured in the observable area.

IV. Conclusion

We formulated a calculation method to estimate the elastic modulus of an extended area of tissue. In addition, we focused on the number of pre-observed deformation patterns and the sparseness of the gradient of tissue elasticity to improve estimation accuracy. As a result, the proposed method of estimation was found to give improved accuracy and proved to be very effective. In conclusion, it was confirmed that the proposed method can estimate spatial variations of the elastic moduli and extend the area of elasticity reconstruction. In future work, we shall use models of organs of more complicated shape and aim to shorten the simulation times.

Acknowledgment

This research was supported by JSPS Grant-in-Aid for Scientific Research (B) (Grant No. 15H03032) and the Center of Innovation (COI) Program of the Japan Science and Technology Agency (JST).

References

[1] J. Ophir, I. Cespedes, H. Ponnekanti, Y. Yazdi, and X. Li, "Elastography: A quantitative method for imaging the elasticity of biological tissues," *Ultrason. Imaging*, vol. 13, no. 2, pp. 111–134, 1991.

[2] T. Shiina, "JSUM ultrasound elastography practice guidelines: Basics and terminology," *J. Med. Ultrason.*, vol. 40, no. 4, pp. 309–323, 2013.

[3] J. McLaughlin and D. Renzi, "Using level set based inversion of arrival times to recover shear wave speed in transient elastography and supersonic imaging," *Inverse Probl.*, vol. 22, no. 2, pp. 707–725, 2006.

[4] M. M. Doyley, "Model-based elastography: a survey of approaches to the inverse elasticity problem," *Phys. Med. Biol.*, vol. 57, no. 3, pp. R35–R73, 2012.

[5] M. Tabaru, T. Azuma, and K. Hashiba, "Measurement of elastic properties of tissue by shear wave propagation generated by acoustic radiation force," *Jpn. J. Appl. Phys.*, vol. 49, no. 7 PART 2, 2010.

[6] O. Goksel, H. Eskandari, and S. E. Salcudean, "Mesh adaptation for improving elasticity reconstruction using the FEM inverse problem," *IEEE Trans. Med. Imaging*, vol. 32, no. 2, pp. 408–418, 2013.

[7] M. Nakao, T. Kuroda, M. Komori, H. Oyama, K. Minato and T. Takahashi, "Transferring Bioelasticity Knowledge through Haptic Interaction", IEEE Multimedia, vol. 13, no. 3, pp.50-60, 2006.

[8] M. Nakao and K. Minato, "Physics-based Interactive Volume Manipulation for Sharing Surgical Process", *IEEE Trans. Info. Tech. Biomed.*, vol.14, No. 3, pp. 809-816, 2010.

[9] R. Sakata, M. Nakao, T. Matsuda, "Estimation of External Forces on the Basis of Local Displacement Observations of an Elastic Body", Advanced Biomedical Engineering, Vol. 6, pp. 21-27, 2017.

[10] A. Saito, M. Nakao, Y. Uranishi and T. Matsuda, "Deformation Estimation of Elastic Bodies Using Multiple Silhouette Images for Endoscopic Image Augmentation," *IEEE International Symposium on Mixed and Augmented Reality (ISMAR)*, pp. 170-171, Sep 2015.

[11] D. L. Valeria, G. Székely, and C. Tanner. "Estimation of Large-Scale Organ Motion in B-Mode Ultrasound Image Sequences: A Survey," *Ultrasound in Medicine & Biology*, vol. 41, pp. 3044-3062, 2015.

[12] N. Hansen, "The CMA evolution strategy: A tutorial," *Vu le*, vol. 102, no. 2006, pp. 1–34, 2011.